Lecture 15: Waves on deep water, II

Lecturer: Harvey Segur. Write-up: Andong He

June 23, 2009

1 Introduction.

In the previous lecture (Lecture 14) we sketched the derivation of the nonlinear Schrödinger equation (NLS)

$$i\partial_\tau A + \alpha\partial_\xi^2 A + \beta\partial_\zeta^2 A + \gamma|A|^2 A = 0, \tag{1}$$

where $\{\alpha, \beta, \gamma\}$ are real constants related to the original physical system from which the NLS was derived. Equation (1) is an important approximate model to describe deep water waves. In probing into the existence of stable wave patterns that propagate with (nearly) permanent form in deep water, we encountered the modulational (or Benjamin-Feir) instability. In most cases, 1D plane wave solutions of the NLS were found to be unstable to 1D perturbations (along the wave propagation axis) and 2D perturbations (transverse to the wave propagation axis).

We continue studying the existence and stability of waves with either 1-D or 2-D surface patterns in this lecture, focusing on more recent work. We discuss two topics: (1) what happens after the initial development of the Benjamin-Feir instability for "high"-amplitude nonlinear plane waves, namely Fermi-Pasta-Ulam (FPU) recurrence (with additional subtleties), and (2) the possible stabilization of "low"-amplitude nonlinear plane waves against the Benjamin-Feir instability by dissipation.

2 Near recurrence of initial states.

Benjamin & Feir [2] showed that a periodic wave train with initially uniform finite amplitude is unstable to infinitesimal perturbations. The instability takes the form of a growing "modulation" of the plane wave, or when viewed in terms of the Fourier spectrum, as exponentially growing sidebands to the plane wave frequency. But this instability is only the beginning of the story: the long-time behavior of such wave trains is arguably even more remarkable.

Lake, Yuen, Rungaldier & Ferguson [10] proposed that with periodic boundary conditions, the focusing 1-D NLS ($\sigma = 1$ in (3)) should exhibit near recurrence of initial states just as the Korteweg-de Vries equation does (see Lecture 5).

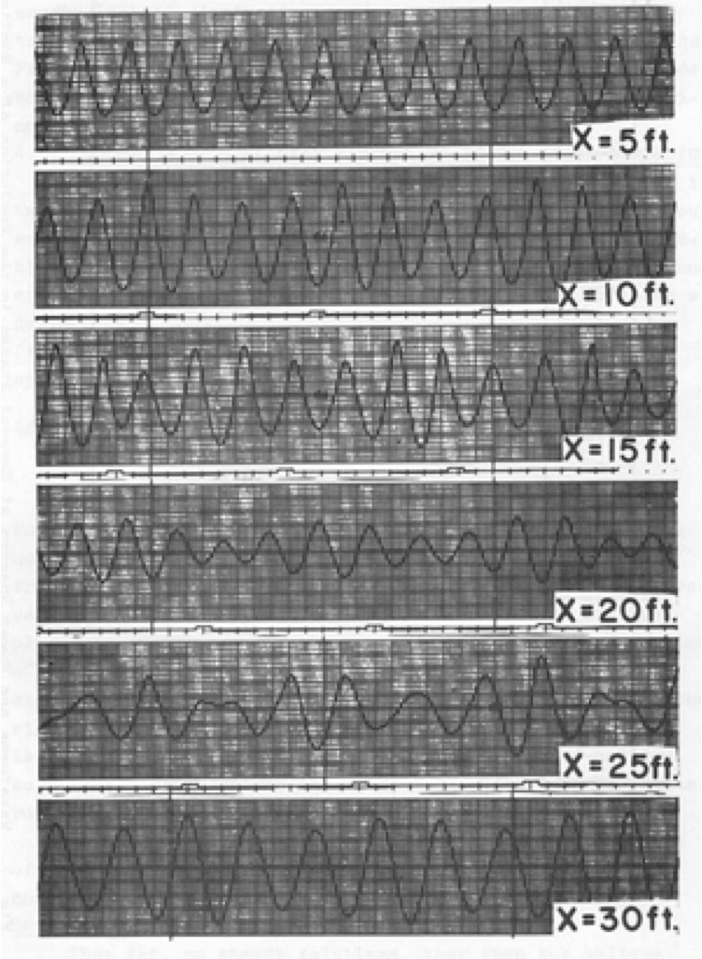

Figure 1: Example of the long-time evolution of an initially nonlinear wave train. Initial wave frequency is 3.6 Hz; oscillograph records shown on expanded time scale to display individual wave shapes; wave shapes are not exact repetitions each modulation period because modulation period does not contain integral number of waves.

To illustrate very qualitatively what "near recurrence of initial states" may mean, we take the linearized equations on deep water with periodic boundary conditions as an example, one solution of which will be

$$\eta(x,t) = \sum_{m=1}^{N} a_m \cos\{mx - \omega_m t + \phi_m\}, \quad \text{where } \omega_m^2 = gm. \tag{2}$$

Since frequencies are not rationally related (recall that $\omega_m = \omega_1\sqrt{m}$), η is not periodic in time. But for functions η that can be written as a sum over a *finite* number N of such terms, the solution returns *close* to its initial state.

The situation for solutions of the NLS is of course different, owing to the nonlinear nature of the equation, but is not entirely unrelated. Just as for the KdV, we saw that

the NLS can be solved using an inverse scattering transform. In the previous lecture, we discussed the case of an infinite domain, which yields, just as for the KdV, a finite number of soliton solutions, each related to a discrete eigenvalue and corresponding eigenmode of the scattering problem. A related scattering problem can be constructed in the periodic domain, and similarly yields a *finite* number of eigenvalues and eigenmodes. Hence, the dynamics of the solutions of the NLS in the periodic domain are limited to understanding the evolution of a finite number of periodic modes. By contrast to the linear case described above, the solution of the NLS is not a linear superposition of these modes, but nevertheless exhibits a similar recurrence phenomenon. This type of long-time behavior, generic to many nonlinear systems (KdV, NLS, ...) was first discovered by Fermi, Pasta & Ulam [5] in numerical experiments, and has become known as the of Fermi-Pasta-Ulam (or FPU) recurrence phenomenon.

Lake *et. al.* [10] investigated experimentally the long-time behavior of nonlinear wave trains generated by a wavemaker in a water tank. During the early stages of evolution, an initially unmodulated wave train develops an amplitude modulation as predicted by the analysis of Benjamin & Feir (see results for $x = 5, 10$ and 15 ft in Figure 1). As the wave train evolves further, the modulation increases in amplitude and the results of their linearized stability analysis no longer apply. However, as the system continues evolving, the wave train is observed to "demodulate" and the wave form returns to a relatively uniform state ($x = 30$ ft in Figure 1). Therefore the recurrence of wave patterns in deep water observed by Lake *et. at.* might be the first physical evidence of the FPU recurrence phenomenon.

3 2-D free surface.

Let us first briefly summarize the results from the last lecture. We saw that the 1D nonlinear Schrödinger equation,

$$i\partial_\tau A + \alpha\partial_\xi^2 A + \gamma|A|^2 A = 0 \tag{3}$$

has one-soliton solution,s as for example

$$A = a\left|\frac{2\alpha}{\gamma}\right|^{1/2} \operatorname{sech}\{a(\xi - 2b\tau)\}\exp\{ib\xi + i\alpha(a^2 - b^2)\tau\}, \tag{4}$$

in the case of $\alpha\gamma > 0$ (a and b are constants). These solutions are envelope solitons. There are also "dark solitons" when $\alpha\gamma < 0$. The dark solitons are a local reduction in the amplitude of a wave train.

The 1D NLS is often rewritten as

$$i\partial_\tau A + \partial_\xi^2 A + 2\sigma|A|^2 A = 0. \tag{5}$$

by a change of variables, with no loss of generality. In that case, envelope solitons occur for $\sigma = 1$ and dark solitons for $\sigma = -1$. The stability of solutions of the 1D NLS to transverse perturbations is studied using the 2D NLS:

$$i\partial_\tau A + \partial_\xi^2 A + \beta\partial_\zeta^2 A + 2\sigma|A|^2 A = 0. \tag{6}$$

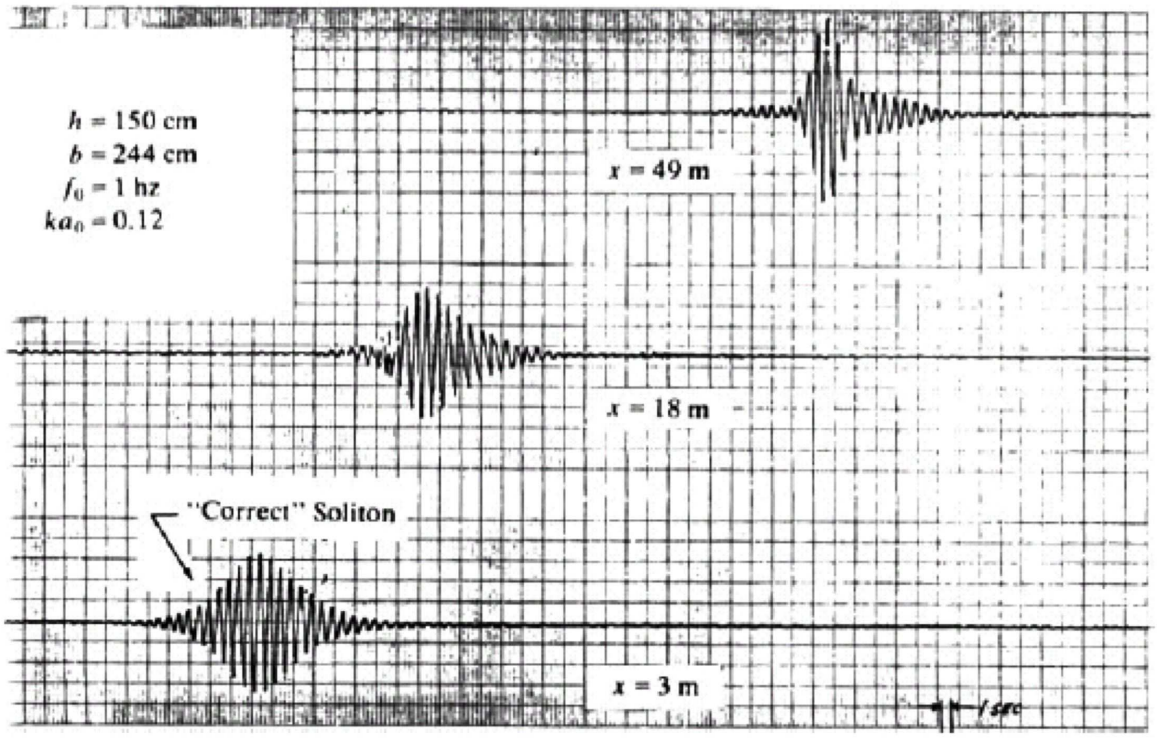

Figure 2: Evolution of water packet in a long tank, showing the transverse instability that was absent in the shorter tank of Figure 2. (Courtesy of J. Hammack)

Zakharov & Rubenchik [12] showed that in the case of $\sigma = 1$, for either sign of β, envelope solitons are unstable to 2-D perturbations; in the case of $\sigma = -1$, for either sign of β, dark solitons are unstable to 2-D perturbations. They also found that the unstable perturbations will have long transverse wavelengths.

As discussed in the previous lecture, Hammack had found "stable" 1D envelope solitons (where the only evolution of the soliton was caused by a weak damping), in apparent contradiction to the aforementioned results. However he later performed additional experiments using the same wavemaker and imposing nearly identical initial conditions, but in a longer tank. It turns out that the longer tank admitted the destabilizing transverse modes that were artificially excluded in the shorter tank, as seen in Figure 2.

Let us now discuss aspects of the 2D NLS which are specific to 2D solutions, first in theory, then in experiments.

Zakharov & Synakh [13] considered the elliptic focusing NLS in 2-D case by choosing $\beta = \sigma = 1$ in equation (6) to obtain

$$i\partial_\tau A + \partial_\xi^2 A + \partial_\zeta^2 A + 2|A|^2 A = 0. \tag{7}$$

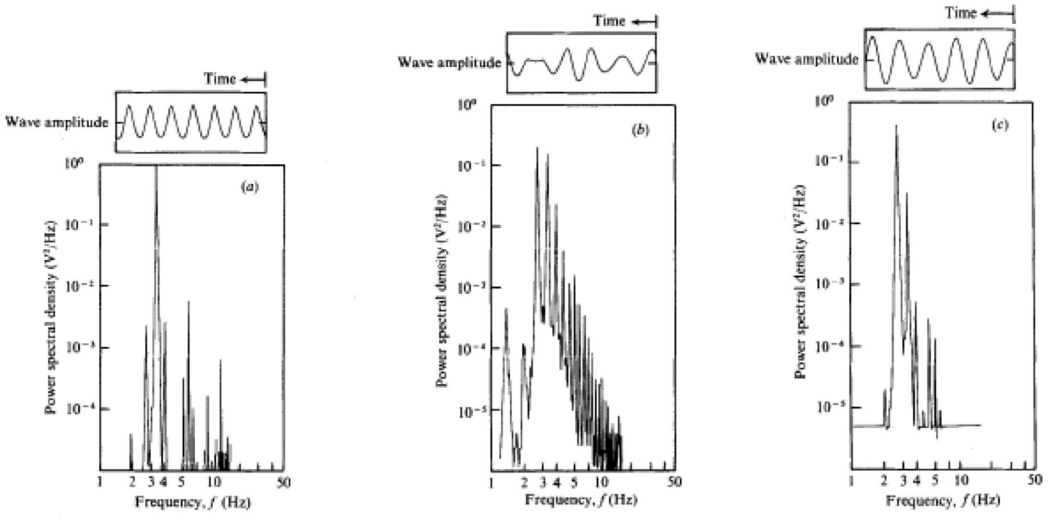

Figure 3: Evolution of a nonlinear finite amplitude wave train: wave forms and power spectral densities vs. propagation distance. (a) Initial stage of side-band growth, $z = 5$ ft, carrier wave with small amplitude modulation. (b) $z = 10$ ft, strong amplitude modulation, energy spread over many frequency components. (c) $z = 25$ ft, reduced amplitude modulation, return of energy to frequency components of original carrier wave, its side bands and harmonics. $f_0 = 3.25$Hz, $(ka)_0 = \delta = 0.23$, $(ka)_{5ft} = 0.29$.

They were able to find the following four conservation laws:

$$I_1 = \int\int (|A|^2) \mathrm{d}\xi \mathrm{d}\zeta, \tag{8}$$

$$I_2 = \int\int (A\partial_\xi A^* - A^*\partial_\xi A) \mathrm{d}\xi \mathrm{d}\zeta, \tag{9}$$

$$I_3 = \int\int (A\partial_\zeta A^* - A^*\partial_\zeta A) \mathrm{d}\xi \mathrm{d}\zeta, \tag{10}$$

$$H = I_4 = \int\int (|\nabla A|^2 - |A|^4) \mathrm{d}\xi \mathrm{d}\zeta. \tag{11}$$

If we consider the function $J(\tau) = \int\int ((\xi^2 + \zeta^2)\,|A|^2) d\xi \mathrm{d}\zeta$, and interpret $|A|^2(\xi, \zeta, \tau)$ as the "mass density", then I_1 is the "total mass" and $J(\tau) \geq 0$ is the "moment of inertia". It follows by direct calculations that

$$\frac{\mathrm{d}^2 J}{\mathrm{d}\tau^2} = 8H, \tag{12}$$

where H is defined in (11). If $H < 0$, $J(\tau)$ will become negative in finite time, and it may happen while quantities I_1, I_2, I_3 and H are kept conserved. This phenomenon, which is so called "wave collapse", has been important in nonlinear optic; nevertheless, since the governing equation (6) (when $\beta = \sigma = 1$) does not apply to the surface-wave case, it is not our major concern in present discussion.

Experiments of 2D NLS wave patterns have revealed a variety of puzzling features. For example, we discussed in Section 2 the notion of FPU recurrence, and its apparent observations in the experiments of Lake, Yuen, Rungaldier & Ferguson [10]. However, a closer

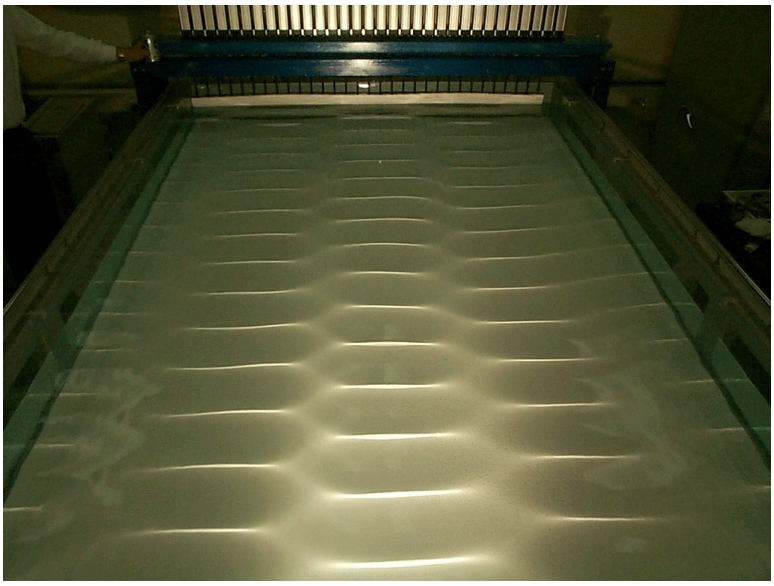

Figure 4: Experimentally stable wave patterns in deep water. Frequency=3Hz, wavelength=17.3cm.

inspection of the results presented in Figure 1 reveals that the period of the recurring pattern increases with distance in the tank (compare the first and last panel), a phenomenon called frequency downshifting. Downshifting has also been observed and studied in optics (see Figure 3, and [6], [7]). Interestingly, however, downshifting does not occur in simulations based on 1-D or 2-D NLS, neither in those based on Dysthe's generalization of NLS ([4]). It remains poorly understood.

In 1990s, Hammack built a new tank to study 2-D wave patterns on deep water. He found experimental evidence, in some situations, of apparently stable wave patterns in deep water (see Figure 4), despite the theoretical results described above [13]. How do we reconcile the experimental observations with Benjamin-Feir instability? There are a few possible explanations.

The first is that the modulational instability only appears in 1-D plane waves, but not in 2-D periodic patterns. Motivated by Hammack's experiments, many researchers began to investigate theoretically the existence of 2-D periodic surface patterns of permanent form on deep water. Craig & Nicholls [3] proved that such solutions are admitted in the full equations of inviscid water waves with gravity and surface tension. Recently, Iooss & Plotnikov [9] proved the existence of such patterns for pure gravity waves on deep water. But neither of these papers considers the stability of the solutions, and the question remains open as to whether they are stable or not.

Another possibility, explored in the next Section, has recently been proposed based on even more puzzling experimental results: Hammack found that conditions on the water surface may be essential for the instability. Figure 5(a) shows a 2D NLS experiment in a tank using recently poured water, which clearly exhibits strong instabilities. Meanwhile using the same volume of water after leaving it sit in the tank for a few days, in exactly

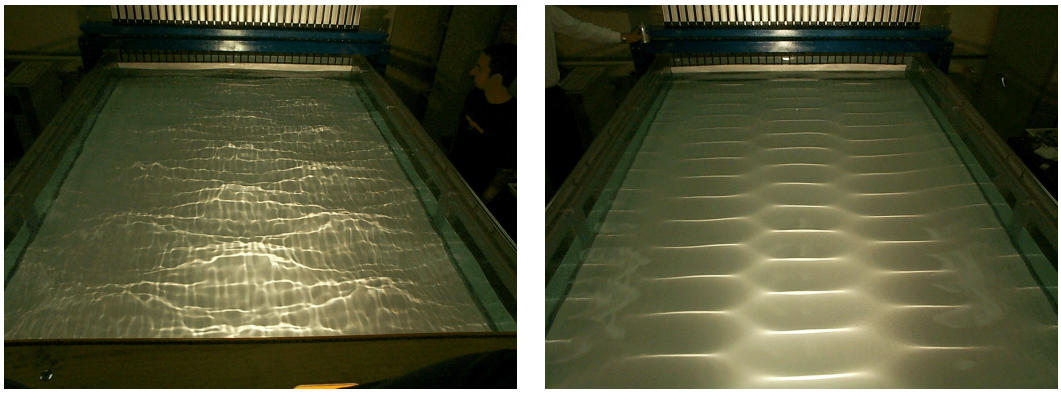

(a) (b)

Figure 5: Surface conditions may play an important role of determining the Benjamin-Feir instability. (a) $f = 2Hz$, new water; (b) $f = 3Hz$, old water.

the same experiment otherwise, reveals the presence of much more stable wave patterns, as shown in Figure 5(b). (For more pictures and movies, visit Pritchard Lab's website at www.math.psu.edu/dmh/FRG). Why should "old" water stabilize the wave pattern? A possible explanation is that impurities accumulating on the water surface provide an additional damping mechanism, to suppress the growth of the slowly-growing modulational instability.

4 Stabilization by damping

To study the possibility of stabilization by damping, let us consider the 1-D NLS with an added damping effect.

$$i(\partial_t A + c_g \partial_x A) + \epsilon(\alpha \partial_x^2 A + \gamma |A|^2 A + i\delta A) = 0, \tag{13}$$

where c_g is the group velocity, ϵ is a small parameter, and δA is the small damping term with $\delta \geq 0$. By introducing variables $\xi = t - \frac{x}{c_g}$ and $X = \epsilon \frac{x}{c_g}$, we obtain

$$i\partial_x A + \alpha \partial_\xi^2 A + \gamma |A|^2 A + i\delta A = 0. \tag{14}$$

Define $A(\xi, X) = e^{-\delta X} \mathcal{A}(\xi, X)$, then (14) becomes

$$i\partial_X \mathcal{A} + \alpha \partial_\xi^2 \mathcal{A} + \gamma e^{-2\delta X} |\mathcal{A}|^2 \mathcal{A} = 0. \tag{15}$$

Equation (15) is in fact a Hamiltonian equation, with a Hamiltonian

$$\hat{H}(X) = i \int \left(\alpha |\partial_\xi \mathcal{A}|^2 - \frac{\gamma}{2} e^{-2\delta X} |A|^4 \right) \mathrm{d}\xi. \tag{16}$$

It follows immediately that $\frac{d\hat{H}}{dX} \neq 0$.

There is a solution to (15) corresponding to a wave train that is uniform in ξ

$$\mathcal{A}_1 = \mathcal{A}_0 \exp\left\{ i\gamma |\mathcal{A}_0|^2 \left(\frac{1 - e^{-2\delta X}}{2\delta} \right) \right\} \tag{17}$$

If we perturb $\mathcal{A}$ around $\mathcal{A}_1$ by setting

$$\mathcal{A}(X,\xi) = \exp\left\{ i\gamma |\mathcal{A}_0|^2 \left(\frac{1 - e^{-2\delta X}}{2\delta} \right) \right\} [|\mathcal{A}_0| + \mu(u + iv)] + O(\mu^2), \tag{18}$$

and insert (4) into (15), then equating $O(\mu)$ terms to zero yields

$$\partial_X v = 2\gamma e^{-2\delta X} |A_0|^2 u + \alpha \partial_\xi^2 u, \tag{19}$$

$$\partial_X u = -\alpha \partial_\xi^2 v \qquad . \tag{20}$$

Without loss of generality, we seek solutions in the form

$$u(X,\xi) = \hat{u}(X) e^{im\xi} + \hat{u}^*(X) e^{-im\xi}, \quad \text{and} \quad v(X,\xi) = \hat{v}(X) e^{im\xi} + \hat{v}^*(X) e^{-im\xi}, \tag{21}$$

where $*$ stands for the complex conjugate. It follows from (19) and (20) that

$$\frac{d^2 \hat{u}}{dX^2} + \left[\alpha m^2 \left(\alpha m^2 - 2\gamma e^{-2\delta X} |\mathcal{A}_0|^2 \right) \right] \hat{u} = 0. \tag{22}$$

By Lyapunov's definition, a uniform wave train solution is said to be *linearly stable* if for every $\epsilon > 0$ there is a $\Delta(\epsilon) > 0$ such that if a perturbation (u, v) satisfies

$$\int [u^2(\xi, 0) + v^2(\xi, 0)] d\xi < \Delta(\epsilon) \quad \text{at } X = 0, \tag{23}$$

then necessarily

$$\int [u^2(\xi, X) + v^2(\xi, X)] d\xi < \epsilon \quad \text{for all } X > 0. \tag{24}$$

It follows that there is a universal bound B which the total growth of any Fourier mode can not exceed. To demonstrate the stability, one can choose $\Delta(\epsilon)$ so that

$$\Delta(\epsilon) < \frac{\epsilon}{B^2}. \tag{25}$$

Using Lyapunov's definition, we can see that there is a growing mode of equation (22) if

$$\alpha m^2 \left(\alpha m^2 - 2\gamma e^{-2\delta X} |\mathcal{A}_0|^2 \right) < 0. \tag{26}$$

It is not difficult to see that the growth stops eventually for any $\delta > 0$. Moreover, the total growth is bounded (see Figure 6.).

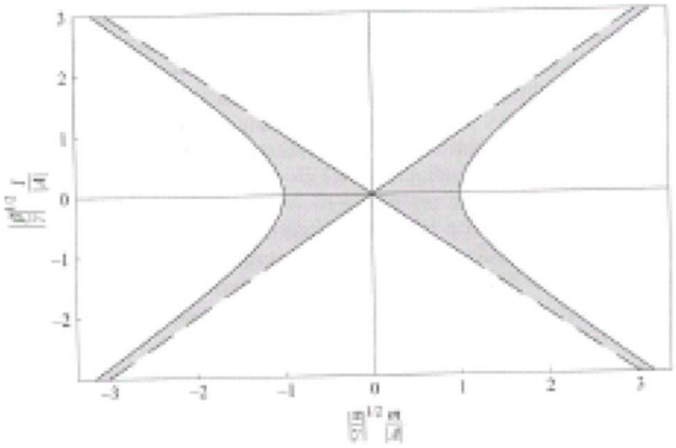

Figure 6: The shaded region shows the location of the growing modes in wavenumber space. The abscissa is $\left|\frac{\alpha}{\gamma}\right|^{\frac{1}{2}} \frac{m}{|A|}$, and the ordinate is $\left|\frac{\beta}{\gamma}\right|^{\frac{1}{2}} \frac{l}{|A|}$. Note that the experimental results presented are for the $\beta = 0$ case.

5 Experimental verification.

We compare the theory presented above with data from a series of experiments ([11]). Figure 7 shows measured water surface displacement in column 1 and modal amplitudes obtained from the corresponding Fourier transforms in column 2, measured at different distance from the wavemaker. At X_1, the Fourier spectrum shows that most of the power is in the carrier wave frequency (at 3.3Hz) and its first harmonic, as well as two small peaks very close to 3.3Hz. These provide a long-wave sinusoidal modulation of the carrier wave, as observed in the left-hand column. As the modulated wavetrain propagates downstream, we observe two changes: its overall amplitude decays, and the shape of the modulation changes. By inspection of the Fourier spectrum, we see that additional sidebands with frequencies near that of carrier wave 3.3Hz have grown between X_1 and X_8

Figure 8 compares the measured and predicted amplitudes of the set of initially seeded sidebands. Since the original Benjamin-Feir analysis did not include dissipation, direct comparison between their non-dissipative theory with the experiments shows very poor agreement (and is not shown in the Figure). A somewhat better agreement, as proposed by Benjamin (1968), can be obtained by calculating the growth rate of the side-bands and subtracting from this estimate their theoretical dissipation rate (which can be deduced from that of the carrier wave, since they nearly have the same frequency). As shown in the Figure 8, the amplitude predictions using this method agree with the experiments for short distances along the tank. However, for longer distances this simple estimate is no longer valid.

A much better agreement is obtained by using the full dissipative theory described above. This experiment thus clearly demonstrates that the stabilization of the side-bands results from the gradual decay of the amplitude of the *carrier* wave by dissipation, which

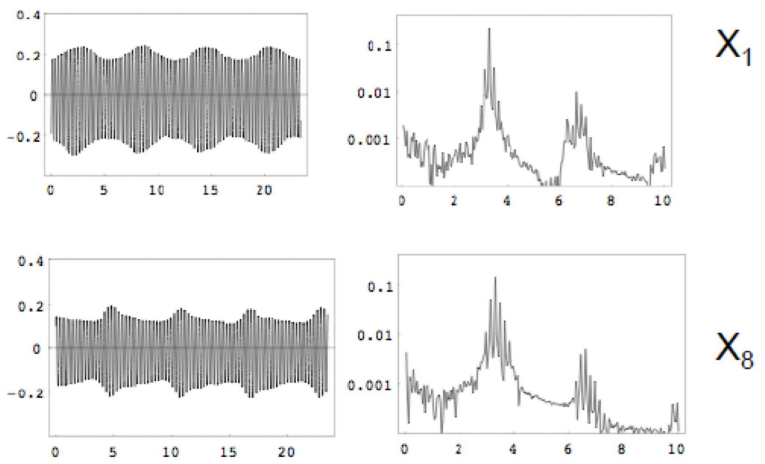

Figure 7: Experimental wave records. Column 1: water displacement (in cm) with time abscissa; column 2: corresponding Fourier coefficients (in cm) with frequency abscissa. Distance of the wave gauge from the wavemaker: 128 cm at X_1, and 478 cm at X_8. See also [11].

in turn stronly reduces the growth rate of the modulational instability.

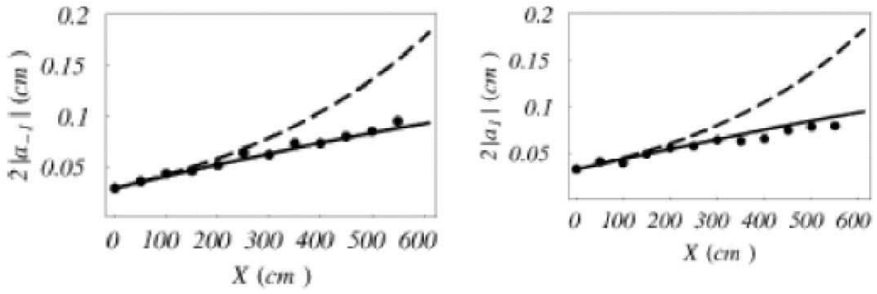

Figure 8: Prediction (solid curves) from the damped NLS theory (22) and measurements (dots) of the amplitudes of the two seeded sidebands $|a_{-1}|$ and $|a_1|$ as functions of distance from the wavemaker. $X = 0$ corresponds to 128 cm from the wavemaker. The dashed line corresponds to the Benjamin-Feir growth rate to which the side-band dissipation rate has been substracted.

The growth of the next two unseeded sidebands are shown in Figure 9. Since none of these were seeded, they started with smaller amplitudes than seeded the ones and remained smaller. Again, the damped NLS theory adequately predicts their evolution.

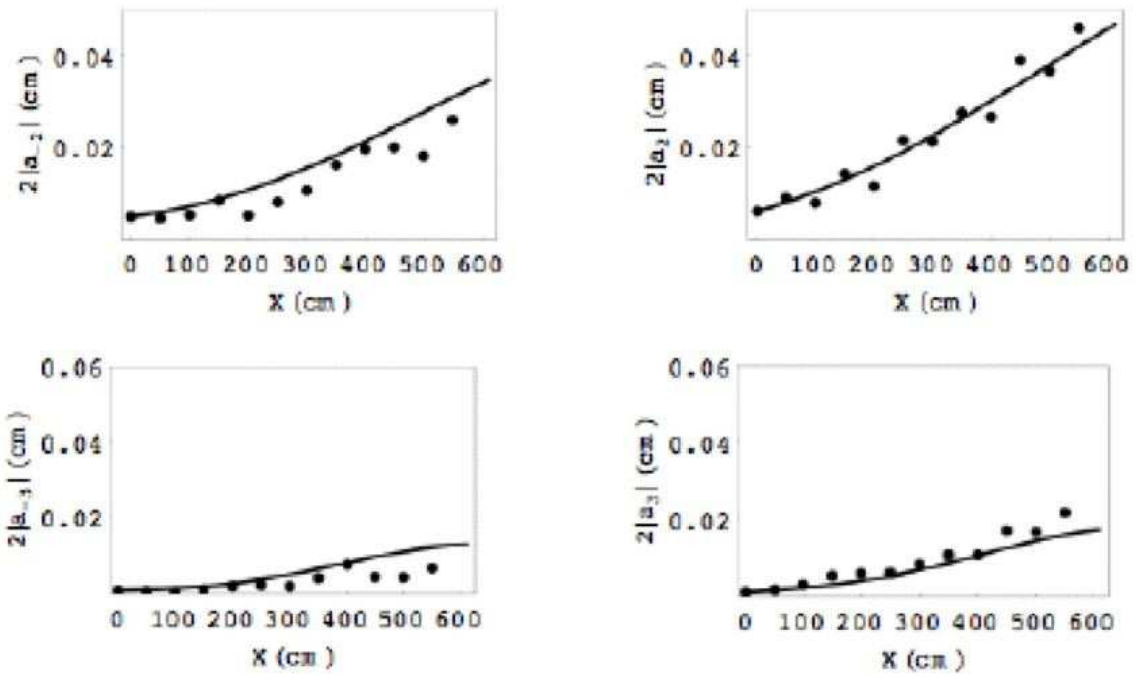

Figure 9: Prediction (solid curves) and measurements (dots) of the amplitudes of the two unseeded sidebands, (a) $|a_{-2}|$ and (b) $|a_2|$, and the amplitudes of the third set of sidebands, (c) $|a_{-3}$ and (d) $|a_3|$, as functions of distance from the wavemaker. $X = 0$ corresponds to 128 cm from the wavemaker, and the starting values of the amplitude were taken from data measured at the $n = 1$ location.

6 Summary.

The Benjamin-Feir instability implies that (1D) stable wave patterns propagating on deep water with nearly permanent form do no exist without presence of damping effects. But any amount of damping of the right kind can stabilize the instability. This dichotomy between with and without damping applies to both 1-D plane waves and to 2-D periodic surface patterns. However, this explanation is still somewhat controversial.

References

[1] M. Ablowitz & H. Segur, *Solitons and the inverse scattering transform*, Society for Industrial Mathematics, (2000)

[2] T. Benjamin & J. Feir, *The disintegration of wave trains on deep water Part 1. Theory*, J. Fluid Mech., **27**, 417, (1967)

[3] W. Craig & D. Nicholls, *Traveling two and three dimensional capillary gravity water waves*, SIAM journal on mathematical analysis, **32**, 2, 323-359, (2000)

[4] K. Dysthe, *Note on a Modification to the Nonlinear Schrodinger Equation for Application to Deep Water Waves*, Proc. R. Soc. Lond. A, **369**, 105-114, (1979)

[5] E. Fermi, J. Pasta & S. Ulam, *Studies of nonlinear problems*, 1940. In Collected Papers of Enrico Fermi, **2**, 978. University of Chicago Press, (1962)

[6] J. Gordon, *Theory of the soliton self-frequency shift*, Optics Letters, **11**, 10, 662-664, (1986)

[7] F. Mitschke & L. Mollenuar, *Discovery of the soliton self-frequency shift*, Optics Letters, **11**, 10, 659, (1986)

[8] A. Hasegawa & Y. Kodama, *Solitons in optical communications* , Clarendon press Oxford, (1995)

[9] G. Iooss & P. Plotnikov, *Small divisor problem in the theory of three-dimensional water gravity waves*, Memoirs of AMS. **200**, No 940, (2009)

[10] B. M. Lake, H. C. Yuen, H. Rungaldier & W. E. Ferguson, *Nonlinear deep-water waves: theory and experiment. Part 2. Evolution of a continuous wave train*, J. Fluid Mech., **83**, 1, 49-74, (1977)

[11] H. Segur, D. Henderson, J. Carter, J. Hammack, C. Li, D. Pheiff & K. Socha, *Stabilizing the Benjamin-Fair instability*, J. Fluid Mech., **539**, 229-271, (2005)

[12] V. Zakharov & A. Rubenchik, *Instability of waveguides and solitons in nonlinear media*, Sov. Phys. JETP, **38**, 494-500, (1974)

[13] V. Zakharov & V. Synakh, *The nature of self-focusing singularity*, Sov Phys JETP, **41**, 441-448, (1976)